19. Amplitude Contrast

Definition of contrast
We can define contrast as the fractional change in intensity:

$$\text{contrast} \equiv \frac{\Delta I}{\overline{I}}$$

This definition emphasizes the intensity difference between points relative to some average intensity. So if the feature can be imaged with the same intensity difference, but upon a lower background intensity, the contrast will be higher. This is usually a good rule of thumb, but it does depend on whether the background arises from noise or actual signal. If the background contains signal with little noise, we can usually subtract it out digitally.

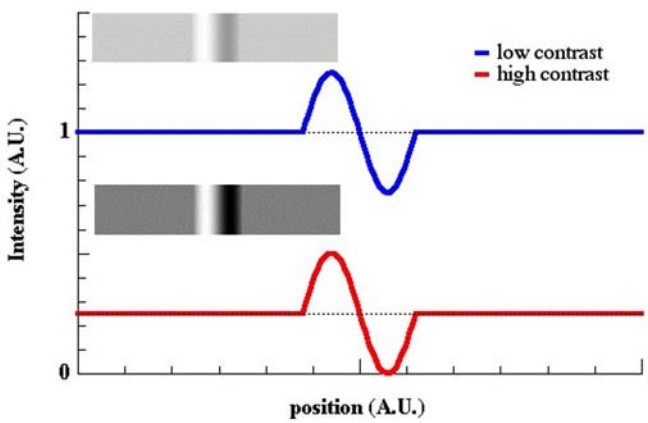

Example: Cellulose + CdSe NPs
Here is an example, if one is needed, of contrast differences. It shows CdSe nanoparticles more-or-less adhering to a strand of cellulose, on a carbon support. The inorganic CdSe is easy to spot, because of the high contrast with respect to the carbon background. The cellulose, on the other hand, looks a lot like the carbon, on slightly darker, mainly due to the added thickness. The main contributions to contrast in this image can be attributed to so-called mass-thickness effects.

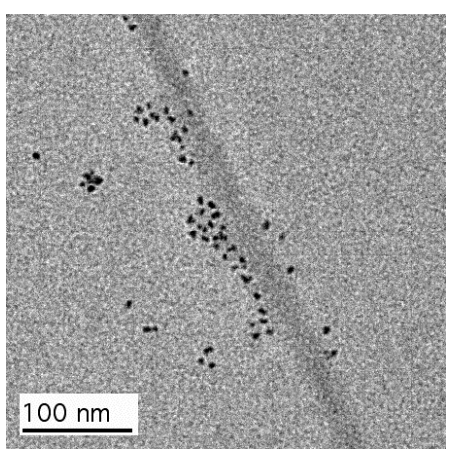

Mass-thickness contrast

Mass-thickness is the primary contrast mechanism for amorphous or organic materials. It results from incoherent, elastic scattering. In our discussion of scattering cross-sections, we found that the intensity varied as

$$I(T) = I_0 \mathrm{e}^{-\mu T}$$

where the attenuation coefficient is

$$\mu = \frac{N_\mathrm{A} \cdot \rho \cdot \sigma_0}{A}$$

The product μT can be regrouped:

$$\mu T = \left(\frac{N_\mathrm{A} \sigma_0}{A} \right) \cdot (\rho T)$$

We call the quantity ρT the *mass thickness* (really mass per unit area, with units of $\mathrm{g/cm^2}$). The ratio in front is not necessarily constant, but Avogadro's number N_A is constant, and we do roughly expect σ_0 to increase with A.

Theorem of reciprocity

The theorists out there are looking for some deeper explanations. There is one that links TEM and STEM, called the theorem of reciprocity. When we draw a ray diagram, for example, for the TEM column, we could, in principle, reverse the direction of the rays, and imagine an exactly opposite situation, where electrons from a point in the image transmit back up the column, converge onto a point on the sample, then radiation back upward toward the electron source. In a sense, we do have that inverted ray diagram in STEM. But now it is the electron probe that converges on the sample. A STEM detector plays the role of the electron source. In fact, different configurations of on-axis BF or annular DF STEM detectors can be thought of as different condenser apertures that we might use in TEM, whereas the condenser aperture in STEM plays a similar role to the objective aperture in TEM.

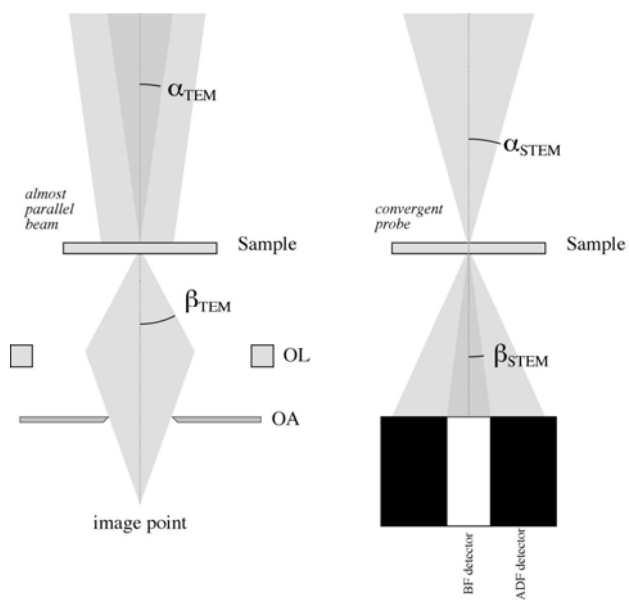

If we follow the analogy, we find that the convergence angle α in TEM replaces β in STEM, and β in TEM replaces α in STEM, and vice versa:

$$\alpha_{TEM} \leftrightarrow \beta_{STEM}$$
$$\beta_{TEM} \leftrightarrow \alpha_{STEM}$$

In other words, if we are able to make these angles match, the STEM contrast would, in principle, be identical to the TEM contrast.

STEM BF/ADF

It should now be apparent that, in comparison to TEM, STEM relies more on different detector geometries to control contrast, rather than different objective apertures or beam tilt. The most common style are on-axis BF detectors and annular DF (ADF) detectors. High-angle annular dark-field (HAADF) detectors have become increasingly popular, for reasons we will discuss in a moment.

Ideally, the deflector lenses in the condenser system raster the beam in a zig-zag pattern over the area of interest. One or more detectors pick up a synchronized signal at each point in the scan to generate the image.

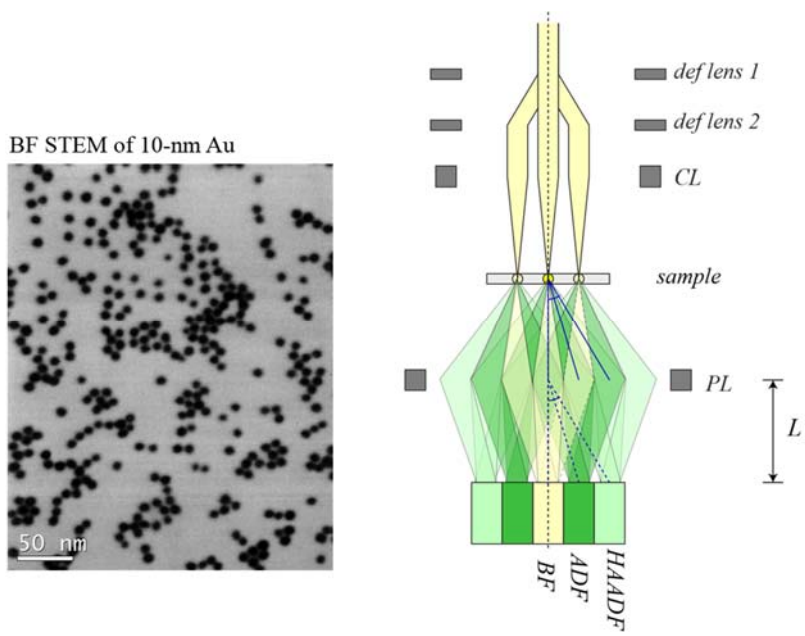

Notice that we want the STEM detectors to see a diffraction pattern from the sample, not an image of the sample. If the shift compensation is adequate, (so that the beam does not tilt while being shifted by the deflector lenses), the diffraction pattern will stay centered on the optic axis, about which the STEM detectors are also centered, as the beam is rastered across the sample. But the diffraction pattern, which is basically a CBED pattern, will be characteristic of each point on the specimen.

Retractable STEM detector

It is useful to have both TEM and STEM components be retractable to allow interchanging between various components along the optic axis. In fact, the component in the column may be only a phosphor that converts the electron signal into a light signal, which is then reflected off a mirror to an optical detector pointing towards radially inwards. This, we can switch between BF and ADF modes using the same detector, although the two signals cannot be detected simultaneously.

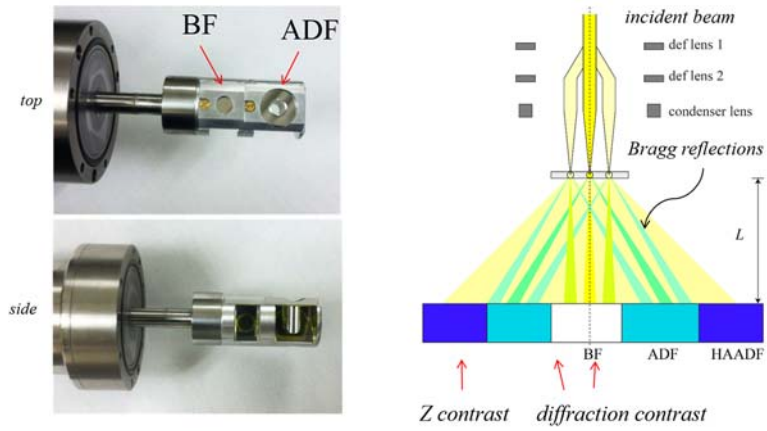

Diffraction contrast

For crystalline materials, especially at low to medium magnification, the most important type of contrast arises from diffraction. Diffraction contrast is a type of amplitude contrast that arises from coherent scattering. It is the contrast generated in BF and centered-DF modes discussed in an earlier chapter. Features like dislocations and defects, chemical interfaces, and structural phases can be selectively highlighted if one knows the correct diffraction conditions to use. A rule of thumb for presentation of diffraction-contrast images from single crystals is to always indicate the direction of the dominant **g**-vector affecting contrast, so that others can correctly interpret the active contrast mechanisms.

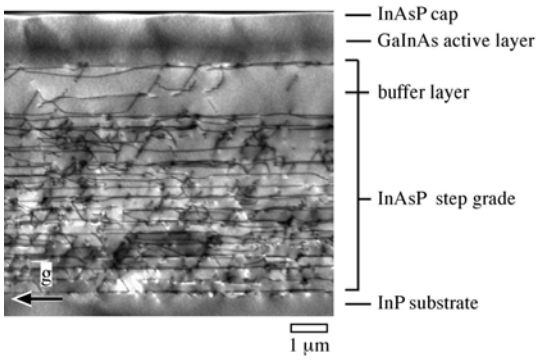

To highlight dislocations using a two-beam condition reveals information about the nature of the dislocations, particularly the direction of their Burger's vector $\mathbf{b}$, a fundamental measure of the type of dislocation. Roughly speaking, the dislocation is invisible if $\mathbf{g} \cdot \mathbf{b} = 0$ in either BF or DF images. In DF images, at a two-beam condition, the dislocation appears dark, because the planes in the vicinity of the dislocation are distorted, so that the Bragg condition as not locally satisfied. So then what do dislocations look like in a BF image using the same reflection g? Also dark. This is because the localized nature of the dislocation in direct space corresponds to a distributed range of scattering in reciprocal space. So the scattered electrons do not end up contributing to either *0* or *g*, but are rather spread into a continuous range of scattering angles in between the diffraction spots.

Diffraction contrast is not always a good thing. For example, we may want to study a feature from different orientations to study its 3-D shape, as in tomography. But even slight changes in orientation from a crystalline sample can cause dramatic differences in contrast.

STEM in an SEM

Many SEMs are also capable of STEM, if they have the right detector. A STEM image of recrystallized Si, acquired on a Zeiss SEM, is shown below. The energies used in SEM are typically much smaller than those in TEM. But diffraction contrast still dominates the image, which features several twin boundaries, with good distinction among the different grain orientations.

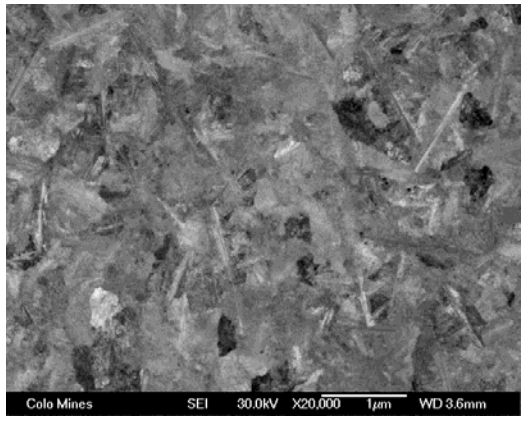

Z-contrast imaging

Z-contrast imaging refers to sensitivity to the atomic number of the constituent elements in a sample. The term is largely associated with HAADF detectors, which pick up the incoherent, elastically scattered electrons at high angles, typically tens of mrad. A major strength of HAADF is that it mostly removes diffraction contrast, while enhancing chemical (i.e., Z) contrast. To do this, it is best *not* to cool the sample. That's because diffraction into high angles increases when a material is cool. You think about it this way: Higher-order reflections correspond to smaller *d* spacings. The temperature is a measure of vibrations in the crystal. The amplitude of vibration increases with T . At high *T*, these small *d* spacings will be essentially averaged out, eliminating the coherent diffraction and revealing the incoherent signal.

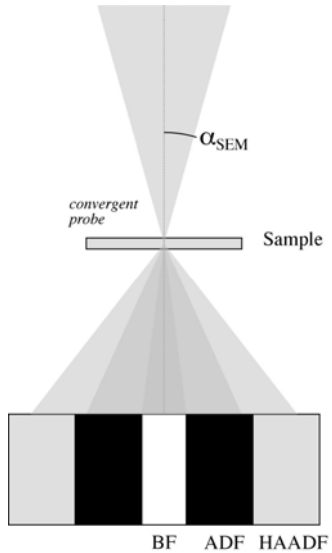

Take the Rutherford model, for illustrative purposes. The form factor was found to be:

$$f_e(\theta) = \frac{\lambda^2 Z e^2 m}{8\pi h^2 \varepsilon_0} \cdot \left[\frac{1}{\sin^2(\theta/2) + \sin^2(\theta_0/2)} \right]$$

We see that at low angle, the screening dominates, giving

$$f_e(\theta) \propto \frac{Z}{\sin^2(\theta_0/2)}$$

At high angle, the screening is negligible, giving

$$f_e(\theta) \propto \frac{Z}{\sin^2(\theta/2)}$$

So does this prove anything? The Z dependence at high angle is fairly clear. We need to look at the low-angle form to compare.

Screening and atomic radius

The size of the atom shows up in a simple model for the screened electrostatic potential. This is the parameter r_0 in the following

$$\varphi(r) = \frac{Ze}{4\pi\varepsilon_0 r} e^{-r/r_0}$$

We found that

$$4\pi \sin(\theta_0/2) = \frac{\lambda}{r_0}$$

If $\lambda \ll r_0$, then assuming then $\theta_0 \approx \lambda/2\pi r_0$. So the low-angle form factor varies as

$$f_e(\theta) \propto Z \cdot r_0^2$$

How does r_0 vary with *Z*? The Bohr model gives an orbital radius for an electron with principle quantum number n of $n^2 \cdot a_B/Z$, in terms of the Bohr radius $a_B = 0.53$ nm, but this neglects the screening effects that arise in multi-electron atoms. Experimentally, screening is minimized within each electron shell, so the sizes of atoms do general decrease from right to left within a particular row of the periodic table, though there is an overall increase from top to bottom. The Thomas-Fermi model, which considers a statistical distribution of electron momentum, predicts that $r_0 \approx a_B/Z^{1/3}$, with an appropriate definition of r_0. This gives a low-angle form factor of

$$f_e(\theta) \propto Z^{1/3}$$

Regardless of the precise form, we expect a weaker, more ambiguous Z dependence of the STEM image contrast using low-angle, ADF imaging, compared to HAADF image. Combined with the coherent diffraction effects at low-angle, HAADF is superior for direct interpretation of chemical contrast.

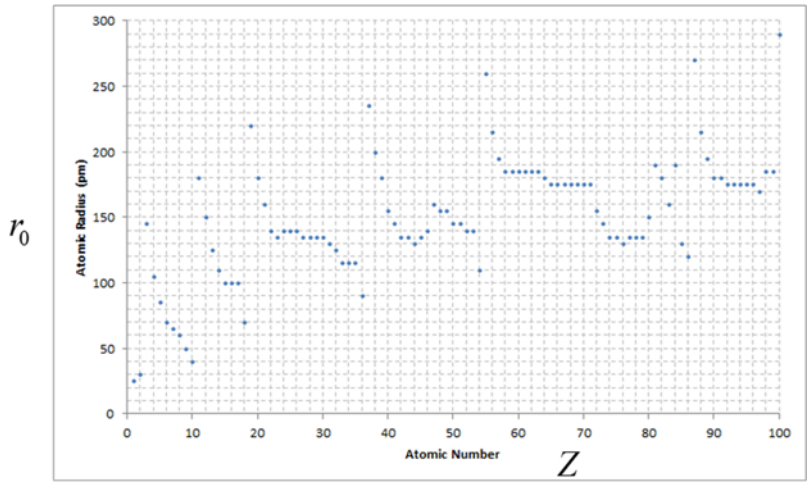

HAADF examples

A couple of examples showing STEM HAADF images are shown below. The first was acquired from InAs nanowires catalyzed with Au nanoparticles. The higher Z of the Au causes the catalysts to appear brighter than the InAs. In normal ADF, we would expect the relative brightness of the Au to depend on the crystal orientation.

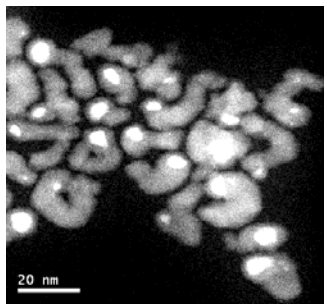
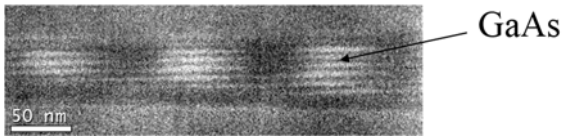
The second example is taken using a regular ADF detector, but shrinking the camera length as much as possible to increase the scattering angle for collected electrons. The image shows GaAs quantum dots in a GaPAs matrix. The contrast results from the higher Z of As compared to P.